Journal of the Serbian Society for Computational Mechanics / Vol. 17 / No. 1, 2023 / pp 71-87
(10.24874/jsscm.2023.17.01.05)

LINEAR AND NON-LINEAR ANALYSES OF PRESSURE PIPE ELBOWS

Benouis Ali[1,2*], Zahi Rachid[3], Moulgada Abdelmadjid[2, 4] and Djebbar Noureddine[2,5]

[1] Faculty of Technology, University of Saida, Bp 138 saida, 20000, Algeria
e-mail: alymoh1980@yahoo.fr
[2] University of Sidi Bel Abbes, Laboratory LMPM, BP 89, City Ben Mhidi, 22000, Algeria
e-mail: alymoh1980@yahoo.fr
[3] Department of Mechanical Engineering, University of Relizane, City Bourmadia, 48000, Algeria
e-mail: zahirachid72@yahoo.fr
[4] Department of Mechanical Engineering, University of Tiaret, city Zaâroura BP 78, Tiaret 14000, Algeria
e-mail: amoulgada@hotmail.fr
[5] Department of Mechanical Engineering, University of Ain Temouchent, BP 101, Ain Temouchent 46000, Algeria
e-mail: djebbarnour@yahoo.fr
**corresponding author*

Abstract

The introduction of pressure piping increasingly requires the use of efficient materials which must withstand both high hydrostatic pressures, high mechanical loads and high thermal gradients. At nuclear power plants, piping systems are subjected to high pressures (up to 60 MPa). The occurrence of cracks and their possible spread is one of the serious risks in the industry. For this reason, elbows are considered critical components of a piping system. Therefore, in order to design and/or qualify a pipe structurally, it is useful to have a reliable evaluation of their structural behavior under different combined loads. The objective of this study is to determine analytical functions for the evaluation of the J integral as a function of crack size, elbow size, and the nature and intensity of loading. This assessment is derived from the numerical results obtained by the WARP3D calculation code exploiting the finite element method (FEM).

Keywords: J-integral, stress intensity factor (SIF), elbow, crack, FEM.

1. Introduction

Given the growing interest in pipeline integrity and its impact on safety and the economy, the literature is full of articles in this area. Thus the current development of scientific research on bends, as evidenced by the different works, has made it possible to develop analytical methods to analyze various problems in fracture mechanics, deduced from the results of numerical simulation. The parameters influencing the results are the geometry and nature of the material.

Research on cracked elbows is not as extensive as that on straight pipes. Fracture tests were carried out on carbon steel bends ASTM-A333 Gr.6 or SA333Gr.6, nominal diameter 200-400 mm with longitudinal cracks. Bending and combined bending with pressure tests were carried out at room temperature by several authors.

Chattopadhyay et al. (2005) experimentally studied and provided an analysis of the J integral and formulated equations for the assessment of circumferential crack opening displacement under internal pressure combined with the moment of a large and small radius elbow, respectively, Rp/Rc=3, Rp/Rc=2. These J-integral and COD-based solutions have been developed using the GE/EPRI (General electric/Electric power research institute) method. Salmi et al. (2019) studied the effect of external circumferential elliptical cracks in transition thickness zone of pressurized pipes using XFEM. Figure 1 shows the 3D mesh of an elbow containing a circumferential crack.

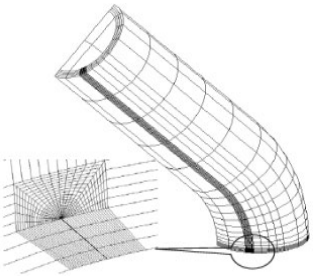

Fig. 1. Representation of the 3D mesh of an elbow containing a circumferential crack Chattopadhyay et al. (2007).

Miller (1988) looked for limit load solutions and studied its influence on the reference stress. Chattopadhyay et al. (2005) also developed analytical expressions for the ovalization of elbow pipes. Mohan et al. (1998) proposed an evaluation scheme of J and COD (Crack Tip Opening Displacement) for elbow pipes. J. Chattopadhyay et al. (2007) conducted experiments on elbows (TWC) 200-400 mm in diameter with circular cracks, subjected to bending loading. Liamani, S et al. (2021) analyzed the presence of a horizontal crack in an HDPE pipe using finite element analysis (FEA) under patch-corrected internal loading. FEA is a computational method employed to simulate and analyze the behavior of structures.

Kim et al. (2006) conducted detailed analyses using the ABAQUS code (2003). They analysed the influence of the crack geometry on the applied load. The stress intensity factors resulting from the current analysis are compared to the existing ones. In addition, their analysis is based on the hypothesis of small deformations and neglecting the effect of geometry change. Miller et al. (1989) stated that for an axial crack at the top of the elbows of a pipe, boundary pressures are not affected by the curvature of the elbow. An evaluation the residual strength of the damaged elbow of the pipeline is carried out on the basis of statistical estimation of the concentration of the stresses and plastic strains of the design with a corrosion defect, given with random dimensions, depending on the time of its occurrence, with a development of a parametric FE model (Larin et al. 2018).

The objective of this study is to evaluate the J integral in relation to the various parameters (crack size, elbow dimensions, intensity and nature of loads).

2. Geometrical model and load

Geometrically, a 90° elbow in a pipe system is characterized by two parameters: the bend radius (Rp) and the ratio of the mean radius to the wall thickness of the elbow (Rc/t).

Ratio of Bend Radius to Wall Thickness (Rc/t):

The ratio Rc/t is used to evaluate the structural integrity and flexibility of the elbow.

The mean radius provides an alternative way to characterize the curvature of the elbow.

The elbow diameter (D) refers to the nominal diameter of the pipe elbow. It represents the size of the pipe in terms of its internal diameter.

The report R_C/t:

R_p: Bend radius;

R_c: Mean radius of elbow;

D: Elbow diameter.

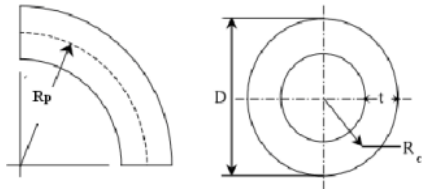

Fig. 2. Elbow geometry.

Element	C	Mn	Si	P	S	Ni	Cr	Al	Cu	V
SA333Gr6 (%)	0.12	0.97	0.28	0.01	0.02	0.08	0.13	0.031	0.08	0.002

Table 1. Chemical composition of an elbow SA333Gr6 (Mukhopadhyay et al. 2012).

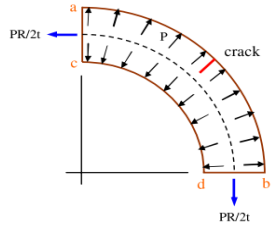

Fig. 3. Elbow loaded with internal pressure.

Description of the geometries studied:

a: Half width of crack.

c: Half length of crack.

t: Thickness of the elbow.

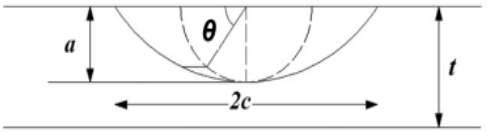

Fig. 4. Angle defining along the crack front (Mechab et al. 2011).

Shape and position of defects:

Normalized by pipe thickness (a/t ratio).

A shape parameter defining the elongation of the elliptic (a/c ratio).

And for $R_c/t=10$;

$$a/t = 0.2\text{-}0.4\text{-}0.6\text{-}0.8$$

$$a/c = 0.8\text{-}0.6\text{-}0.4\text{-}0.2$$

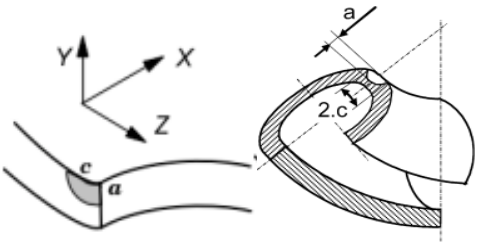

Fig. 5. Internal and external circumferential defect (Kim et al. 2005).

3. Results and discussion

In order to have the information on the behavior of cracks and their impact on the structural integrity of a pipe bend, facilitating decision-making processes related to crack growth, repair strategies and reinforcement techniques, we have numerically calculated the J-integral. In addition, the aim was to obtain analytical functions that can be used as tools for predicting and evaluating the values of the J-integrals analytically for different ratios (Rp/Rc, a/c and a/t), aiding in the design and evaluation of bends under various loading conditions.

3.1 Linear behavior

3.1.1 The elastic contour integral J_e

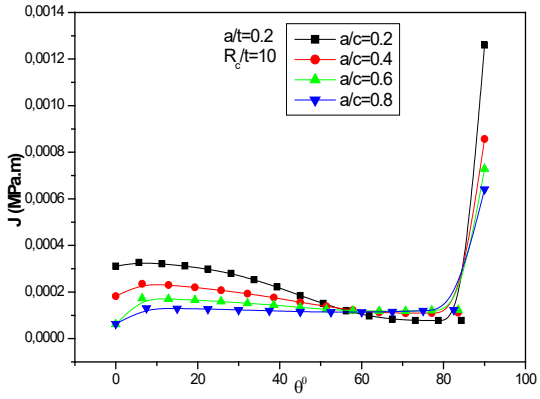

Fig. 6. Variation of contour integral as a function of angle θ°.

Note that the maximum value of the J-integral is obtained at the position θ°=90, regardless of the ratio a/c. This position corresponds to the tip of the crack where the stress concentration is high. We note that the J values are inversely proportional to the a/c ratios; and more the a/c decreases, the more the peak is accentuated and therefore the stress concentration is greater.

3.1.2 The stress intensity factor K_I

The stress intensity factor (SIF) in elastic behavior is related to the J integral by the relation: (Ainsworth et al. 1984).

$$J_e = \frac{K_I^2}{E'} \tag{1}$$

Hence:

$$K_I = \sqrt{J_e E'} \tag{2}$$

With:

$$E' = E \text{ in plane stresses} \tag{3}$$

$$E' = \frac{E}{1-\nu^2} \text{ in plane deformations} \tag{4}$$

Where:

J_e: Elastic contour integral;

K: Stress intensity factor;

E: Young Module;

υ: poison Coefficient.

The stress intensity factor values in Fig.6 allow us to calculate the form factor using the following relationship (Mechab et al. 2018):

$$K_I = \sigma_t \sqrt{\pi \frac{a}{Q}} . F_b \tag{5}$$

With:

$$Q = 1 + 1.464 \left(\frac{a}{c} \right)^{1.65} \quad \text{for} \quad \frac{a}{c} \leq 1 \tag{6}$$

The yield stress defined in following equation (Miller 1988):

$$\sigma y = \frac{P.R}{2.t} \tag{7}$$

Where:

σ_y : Yield stress;

: Newman correction;

F_b: Form factor;

P : Internal pressure;

R: mean radius radius of the elbow.

From equation (5), the form factor can be deduced:

$$F_b = \frac{K_I}{\sigma_t \sqrt{\pi \frac{a}{Q}}} \tag{8}$$

Figure 7 shows the variations in the shape factor as a function of the a/t ratio for different R_P/R_C ratios.

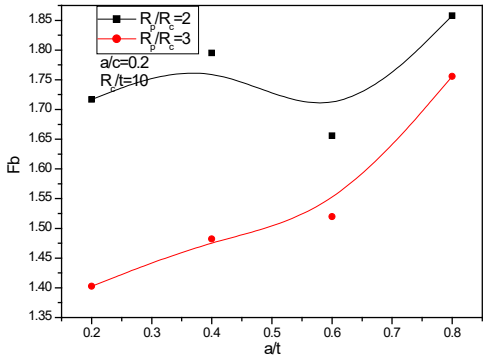

Fig. 7. Variation of the form factor as a function of the a/t ratio for different R_P/R_C ratios for a/c=0.2.

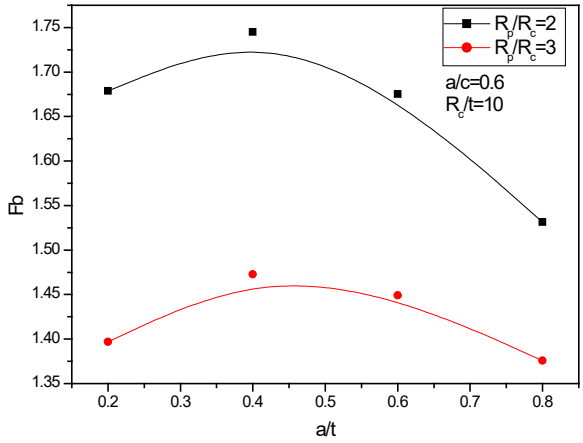

Fig. 8. Variation of the form factor as a function of the a/t ratio for different R_P/R_C ratios for a/c=0.6.

3.1.3 Analytical functions

It is necessary to look for a relationship describing the factor F as a function of the size of the semi-elliptical crack in relation to the thickness of the structure (a/t), in the form of a third-degree polynomial of the form:

$$F_b = B_1\left(\frac{a}{t}\right)^3 + B_2\left(\frac{a}{t}\right)^2 + B_3\left(\frac{a}{t}\right) + B_4 \tag{9}$$

Where: (*Bi*) constants are a function of crack size (a/c).

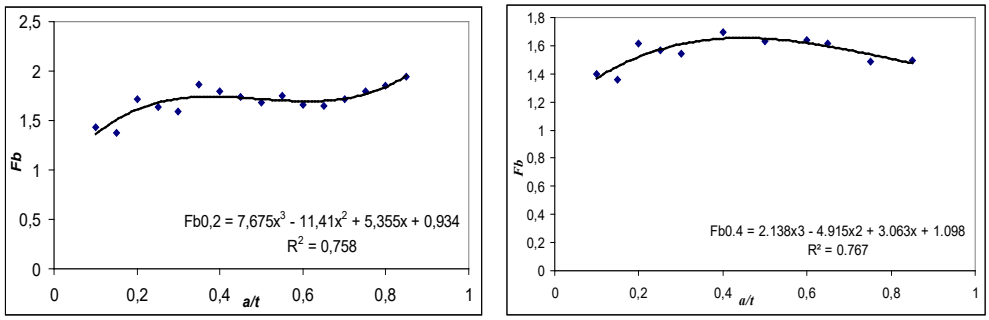

Fig. 9. Representation of the function F_b according to a/t for a/c=0.2, and a/c=0.4.

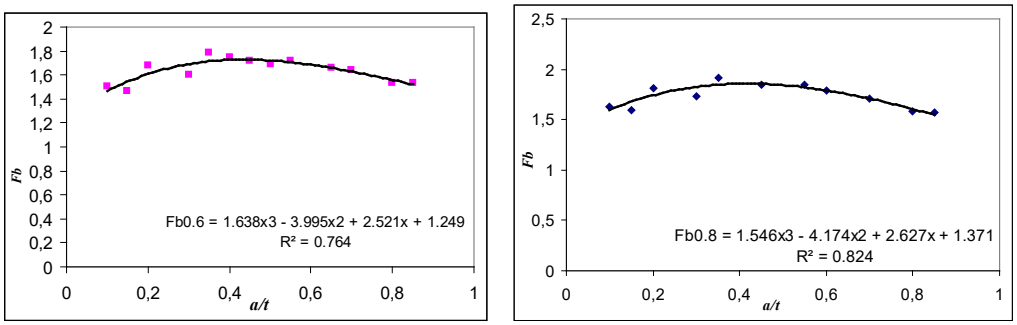

Fig. 10. Representation of the function F_b according to a/t for a/c=0.6 , and a/c=0.8.

Smoothing of the curves allows us to determine that the third degree polynomial gives both an acceptable precision and a simple usable formula.

The B_i coefficients are given by the following formulae: With four (04) values a/c = 0.8, 0.6, 0.4, 0.2;

$$B_1 = -96.483\left(\frac{a}{c}\right)^3 + 178.76\left(\frac{a}{c}\right)^2 - 107.93\left(\frac{a}{c}\right) + 22.883 \tag{10}$$

$$B_2 = 93.431\left(\frac{a}{c}\right)^3 - 181.91\left(\frac{a}{c}\right)^2 + 115.5\left(\frac{a}{c}\right) - 27.989 \tag{11}$$

$$B_3 = -22.971\left(\frac{a}{c}\right)^3 + 49.44\left(\frac{a}{c}\right)^2 - 34.691\left(\frac{a}{c}\right) + 10.5 \tag{12}$$

$$B_4 = -0.3646\left(\frac{a}{c}\right)^3 + 0.285\left(\frac{a}{c}\right)^2 + 0.7491\left(\frac{a}{c}\right) + 0.7762 \tag{13}$$

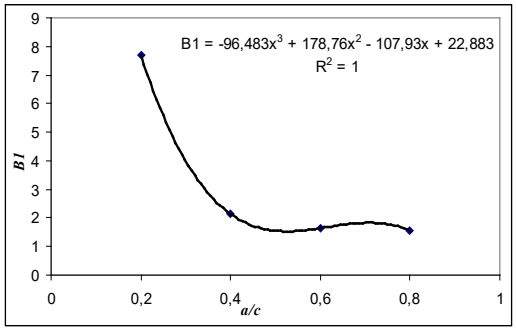

Fig. 11. Representation of the function B_1 according to a/c.

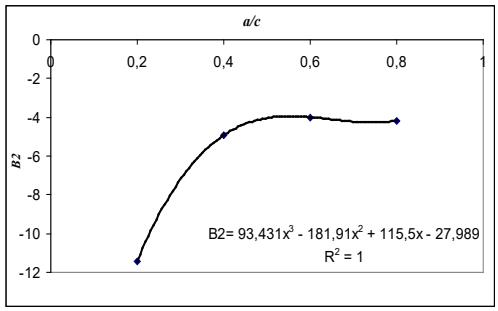

Fig. 12. Representation of the function B_2 according to a/c.

(a) R_p/R_c=3

a/c=0.2						
Rc/t	a/t=0.3			a/t=0.7		
	Fb	FN	E(%)	Fb	FN	E (%)
10	1.612	1.451	9.965	1.859	1.755	5.573

a/c=0.6						
R_c/t	a/t=0.3			a/t=0.7		
	Fb	FN	E(%)	Fb	FN	E (%)
10	1.607	1.396	13.074	1.576	1.678	6.495

(b) Rp/Rc=2

a/c=0.2						
R_c/t	a/t=0.3			a/t=0.7		
	Fb	FN	E (%)	Fb	FN	E (%)
10	1,72436	1,5868	8,6680	1,73524	1,7142	1,2266

a/c=0.6						
R_c/t	a/t=0.3			a/t=0.7		
	F_b	F_N	E(%)	F_b	F_N	E (%)
10	1,6919	1,605	5,392	1,6371	1,6412	-0,2541

Table 2. Comparison between analytical FN and numerical Fb results for R_p/R_c (3, 2), for different ratios a/c (0.2, 0.6).

Table 2 represents a comparison between analytical results (FN) and numerical results (Fb), with the ratio Rp/Rc for values of 3 and 2 and the ratio Rc/t=10, with a/t= (0.3, 0.7). Additionally, the comparison is made for different ratios of a/c= (0.2, 0.6).

This results that the formulae obtained initially for a ratio Rp/Rc = 3 are applicable for the ratio Rp/Rc = 2. One can thus conclude that the ratio Rp/Rc has no influence on the form factor.

We have illustrated in Fig. 13 the variation of the integral J obtained analytically and numerically according to the pressure P and this for ratios a/c, a/t and Rc/t with (a/c=0.4 a/t=0.4 Rc/t=10).

The two curves have points that are almost close and the difference is almost negligible for low pressures, hence certain compatibility between the analytical study and the numerical one. In contrast, the difference increases proportionally with the increase in pressure.

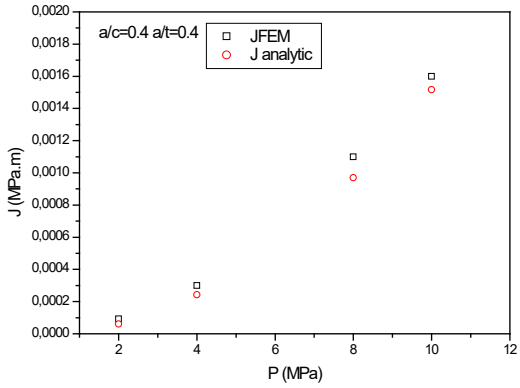

Fig. 13. Representation of the variation of J_e as a function of pressure P (MPa) for a/c=0.4 and a/t=0.4.

The analysis of the variations of J integral shows an approximate agreement between the analytical and numerical results by varying the loading P. The average deviation does not exceed 5.65%.

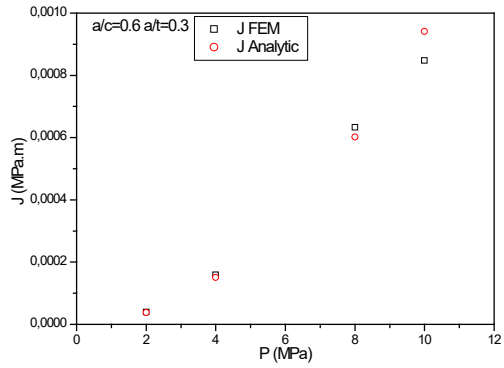

Fig. 14. Representation of the variation of J_e as a function of pressure P (MPa) for a/c=0.6 et a/t=0.3.

In Fig. 14, we analysed the variation of the J integral as a function of loading for the ratio a/c=0.6 and a/t=0.3. We note that the difference between the values is not great with a maximum deviation equal to 3%.

3.2 Non-linear behavior

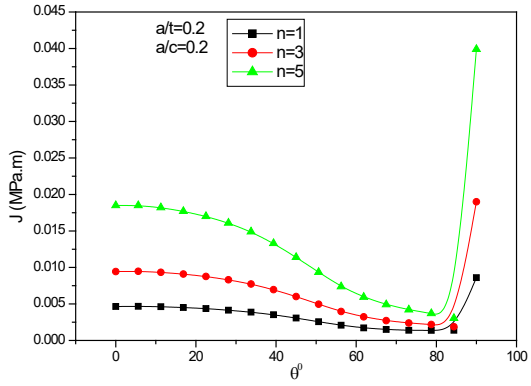

Fig. 15. Variation of the J integral as a function of the angle θ for n=1, 3 and 7.

In Fig. 15, the variation of the J integral as a function of the angle θ is presented for different values of n (1, 3, and 7). The J integral is being used to characterize the effect of the work hardening coefficient on a material with elasto-plastic behavior.

From the results shown in Fig. 15, it is observed that regardless of the material's behavior, the maximum value of the J integral occurs at the crack tip (θ=90°). This indicates that the highest stress intensity is concentrated at the crack tip.

The difference of the values of the integral J for different work hardening coefficients (n) for angles less than 80° are distinct.

To characterize the effect of the work hardening coefficient on the J integral of a material with elasto-plastic behavior, we studied the variation of the J integral along the contour of the crack. The results are shown in Fig. 15. We find that whatever the behavior of the material, the maximum value is at the crack tip (θ=90°). The difference between the values of the J integral is not visible enough for different work hardening coefficients (n), it is of the order 10-4 because the a/t ratio is small.

3.2.1 Load influence on J-integral

The variations of J Integral as a function of pressure (P) are shown in Fig. 16 and Fig. 17 as a function of n. The coefficient n has an influence on the stress concentration at the crack head.

The latter depends on the loading P, the relative dimensions of the crack defined by the ratio a/t at the crack tip. Thus for a/c constant we note that for P weak, the influence of n on J is negligible. When P increases, the influence of n depends on the ratio a/t. and a/t is great, we conclude that the influence of n manifests itself at low pressures.

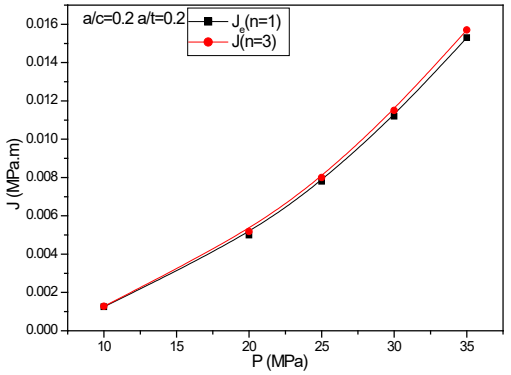

Fig. 16. Variation of J integral as a function of pressure P for a/t=0.2, a/c=0.2.

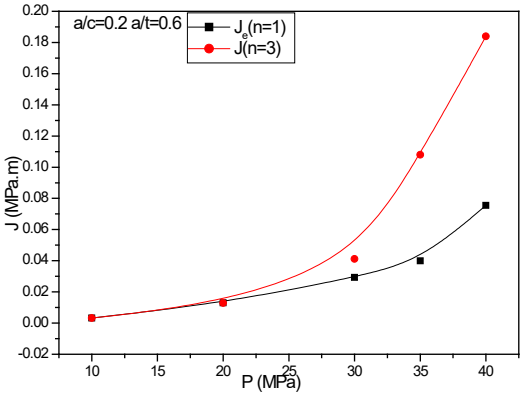

Fig. 17. Variation of J integral as a function of pressure P for a/t=0.6, a/c=0.2.

3.2.2 Determination of functions h(n)

The division of the J-integral into elastic and plastic components allows for a more detailed analysis of crack behavior and the contributions of elastic and plastic deformation to crack growth.

Conventionally, this J integral can be broken down into two terms: (Jae Kim et al. 2002, Lee et al. 2006)

$$J = J_e + J_p \tag{14}$$

$$\frac{J_p}{J_e} = h(n).\left(\frac{P}{P_L}\right)^{n-1} \text{ and } J_p = K.J_e \tag{15}$$

Where:

J_p : Plastic contour integral,

J : Total contour integral,

P_L : Limit pressure,

K: Correction factor,

$h(n)$: Adimensional plasticity function.

The ratio of elastic J-integral to plastic J-integral can vary depending on the pressure ratio and the nature of the material itself, including its pressure resistance and plasticity. These variations can have an impact on crack propagation resistance and the material's ability to absorb energy in an elastic or plastic manner.

3.2.3 Limit pressure on circumferential crack

For this analysis, the choice of material was made on carbon steel with elastoplastic behavior and widely used for the construction of the bends of a pipe with flow limit σ_y*=300MPa*. This structure contains a crack on the outer circumferential part. For such a crack, the limit pressure P_L is given by the following relation obtened by the equation (7) (Miller 1988):

$$P_L = \frac{\sigma_y.2.t}{R} \tag{16}$$

From the relation (15), we deduce h(n). The following figures illustrate the variations of h(n) according to the ratio P/PL for different n.

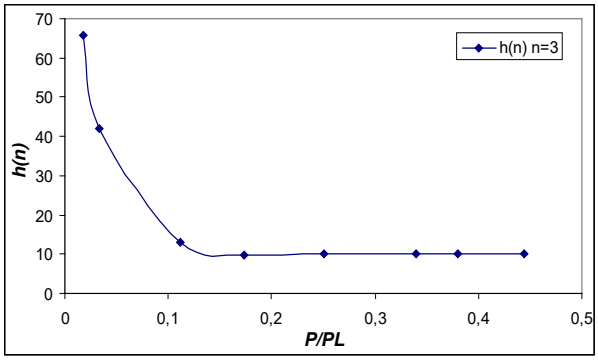

Fig. 18. Variation of function h(n) by ratio (P/PL) for n=3.

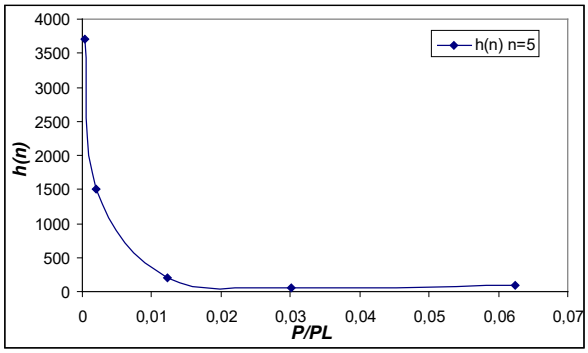

Fig. 19. Variation of function h(n) by ratio (P/PL) for n=5.

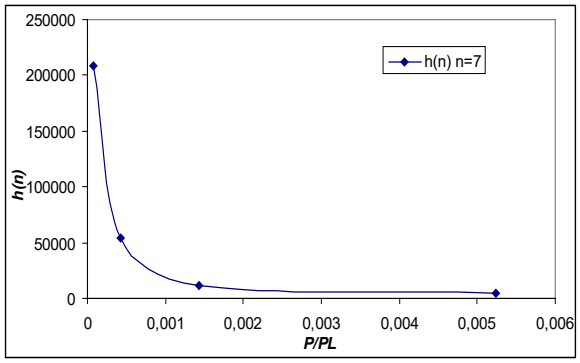

Fig. 20. Variation of function $h(n)$ by ratio (P/P_L) for n=7.

Figures 18, 19, and 20 show the variation of the h(n) function as a function of the pressure ratio applied to the threshold pressure (P/P_L). We note that an increase in this ratio results in a decrease in the h(n) function. It should be noted, however, that this behavior is similar to that found in another study using a wall of constant thickness (Chattopadhyay et al. 2007, Kim et al. 2005). The results shown in these figures make it possible to determine for each pressure applied the value of the function h(n) whatever the size of the crack to calculate the J integral.

We observe that beyond a value of the P/PL ratio, h(n) takes a constant value depending on the number n.

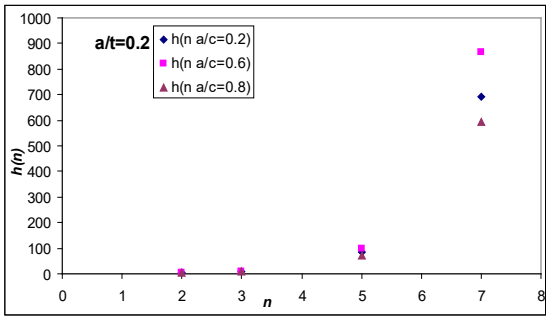

Fig. 21. Variation of the function h(n) in function n for different ratios a/c.

Smoothing of these curves allows us to determine h as a function of n in polynomial form: $h(n)$

$$h(n) = 14{,}558n^3 - 133{,}15\,n^2 + 395{,}74\,n - 371{,}98 \tag{17}$$

In summary, the determination of J according to the loading P and the dimensions of the crack determined by the ratio a/t and a/c and the ratios Rp/Rc; R/t characterizing the elbow has for expressions the following formula:

$$\text{For } P/P_L \leq 0.35 \quad J = 1.17.J_e \tag{18}$$

$$\text{For } P/P_L > 0.35 \quad J = h(n).J_e.(P/P_L)^{n-1} \tag{19}$$

Results give average agreement with 13% error.

The results give an average agreement with an error of 9%.

4. Conclusions

This paper has two components:

An analysis of the breaking behavior of elbows under pressure loading using the concept of J integral exploiting the calculation code Warp3D using the finite element method.

The analysis is based on the elbow geometry and the size of the crack and the behavior of the elastic and elasto-plastic materials; the following results were obtained:

The larger the crack size, the higher the J integral value.

The more the ratio a/c decreases, the more J integral increases;

The greater the radius of curvature, the smaller the J integral.

J integral grows with increased internal pressure.

The maximum J integral value is obtained at the crack head.

In the case of elasto-plastic behavior, the limit pressure stress for its more simplified form was chosen from among the different reference stress definitions, which allowed us to evaluate the correction function h(n) and provide a formula for evaluating the J integral.

The analytical results were compared to the numerical results with good concordance.

References

Chattopadhyay J, Acharyya S, Kushwaha H.S, (2007). Elastic–plastic J and COD estimation schemes for 90◦ elbow with throughwall circumferential crack at intrados under in-plane opening moment, International Journal of Fracture, 144 (4), 227-245.

Chattopadhyay J, Pavankumar T.V, Dutta B.K, Kushwaha H.S, (2005). Fracture experiments on throughwall cracked elbows under in-plane bending moment: Test results and theoretical/numerical analyses, Eng Fract Mech, 72(10), 1461– 1497.

Chattopadhyay J, Tomar A.K, Dutta B.K, Kushwaha H.S, (2005). Elastic-plastic J and COD estimation schemes for throughwall circumferentially cracked elbow under in-plane closing moment, EngFractMech, 72, (14), 2186-2217.

Liamani, S., & Abderahmane, S. (2021). Modeling the Repair of a Crack in an HDPE Pipe. Periodica Polytechnica Mechanical Engineering, 65(2), 134-140.

Kim Y.J, Oh C.S, (2006). Limit loads for pipe bends under combined pressure and in-plane bending based on finite element limit analysis, Int J Press Vessels Piping, 83, 85–90.

Kim Y.J, Shim D.J, (2005). Relevance of Plastic limit load to reference stress approach for surface cracked cylinder problems, International Journal of Pressure Vessels and Piping, 82, 687-699.

Ainsworth R.A., (1984). The assessment of defects in structures of strain hardening materials. Eng. Fract. Mech. 19(4), 633–642.

Mechab, B, chioukh, N, Mechab, B, et al. (2018). Probabilistic fracture mechanics for analysis of longitudinal cracks in pipes under internal pressure. Journal of Failure Analysis and Prevention, vol. 18, p. 1643-1651. (https://doi.org/10.1007/s11668-018-0564-8)

Larin O, Potopalska K, Mygushchenko R, (2018). Statistical Estimation of Residual Strength and Reliability of Corroded Pipeline Elbow Part Based on a Direct FE-Simulations, Journal of the Serbian Society for Computational Mechanics, 12,1,80-95. (DOI: 10.24874/jsscm.2018.12.01.06)

Mechab, B, Serier, B, Bachir Bouiadjra B, Kaddouri K, Feaugas X, (2011). Linear and non-linear analyses for semi-elliptical surface cracks in pipes under bending, International Journal of Pressure Vessels and Piping, 88, 57-63.

Miller A.G, (1988). Review of limit loads of structures containing defects, Int J Press Vessels Piping, 32, Issues 1-4, 197–327.

Miller A.G, Ainsworth R.A, (1989). Consistency of numerical results for power law hardening materials and the accuracy of the reference stress approximation. J, EngFractMech, 32, 237–247.

Mohan R, Krishna A, W.Brust F, Wilkowski G.M, (1998). J-estimation schemes for internal circumferential and axial surface cracks in pipe elbows, Press Vess Technol, 120(4), 418-423.

Mukhopadhyay C.K, Sasikala G, Jayakumar T, Raj Baldev, (2012). Acoustic emission during fracture toughness tests of SA333 Gr.6 steel, Engineering Fracture Mechanics, 96, 294–306

Salmi H, El Had K, El Bhilat H, Hachim A, (2019). Numerical Analysis of the Effect of External Circumferential Elliptical Cracks in Transition Thickness Zone of Pressurized Pipes Using XFEM, J. Appl. Comput. Mech., 5(5), 861-874

Kim Y. Jae, Shim D.J., Choi J.B and Kim Y. Jin, (2002). Elastic-plastic analyses for surface cracked plates under combined bending and tension. The. J. Strain Anal. Eng. Des. 37(1), 33–45

Lee, S.M., Chang, Y.S., Choi, J.B. and Kim, Y.J. (2006). Failure probability assessment of wall-thinned nuclear pipes using probabilistic fracture mechanics, Nucl. Eng. Des, 236, pp. 350-358. DOI:10.1016 /j.nucengdes.2005. 09.008.